Experimental validation of a Pulsating Heat Pipe transient model during the start-up in micro-gravity environment

Mauro Abela[1], Mauro Mameli[1], Vadim Nikolayev[2], Sauro Filippeschi[1]
[1]DESTEC, University of Pisa, Largo L. Lazzarino, Pisa,Italy.
[2]Université Paris-Saclay, CEA, CNRS, SPEC, 91191 Gif-sur-Yvette Cedex, France.

E-mail: mauro.abela@phd.unipi.it

Abstract. A large diameter Pulsating Heat Pipe (PHP) is a device operating as a thermosyphon on ground and as a PHP under microgravity conditions. Such a prototype with a transparent (sapphire) tube section in the adiabatic region has been tested during the 67th ESA parabolic fligH campaign. Infrared visualizations of the fluid in the sapphire section along with measurements of all the relevant quantities, which characterize the device state (pressures, temperatures), are acquired during the tests and exploited for the validation of CASCO code. After accurate implementation of the PHP geometry and material properties, transient simulations have been carried out. A comparison with the experiment is possible for one case where the initial PHP state. The transients for tube wall temperatures, slug velocities, slug length and liquid temperatures show a good agreement with the experiments during the start-up phase in microgravity conditions reducing the gap towards the development of a fully validated PHP design tool.

1. Introduction

The use of PHPs under weigHlessness have been discussed since long time [1] [2]. A PHP with a channel of a large diameter (larger than the critical diameter defined for the Earth gravity) can be more advantageous because of small viscous losses. It remains a capillary in the weigHlessness so is expected to function as a PHP there. Such a device acts however as a loop thermosiphon on Earth [3]. In this work we test such a device during a parabolic fligH (20 s of microgravity) and compare the experimental results to the numerical simulations performed with the CASCO software (French abbreviation for Code Avancé de Simulation du Caloduc Oscillant, Advanced PHP Simulation Code) [4] [5] [6].

2. Experiment

The device designed by the University of Pisa is a closed loop aluminum tube with an inner and outer diameter of 3mm and 5mm, respectively, folded in a 14 turns configuration (Fig. 1) and partially filled with 22ml of FC-72 (50% volumetric filling ratio). An aluminum heat spreader brazed on the tube is heated by two ceramic Joule heaters thus forming the evaporator zone. Two spreaders brazed on the tube are cooled down using a Peltier cell system coupled with a temperature regulation system that imposes Tc=20°C condenser

temperature. One tube section is made of sapphire glass to observe the flow pattern and temperature with the IR camera and high-speed grey-scale camera.

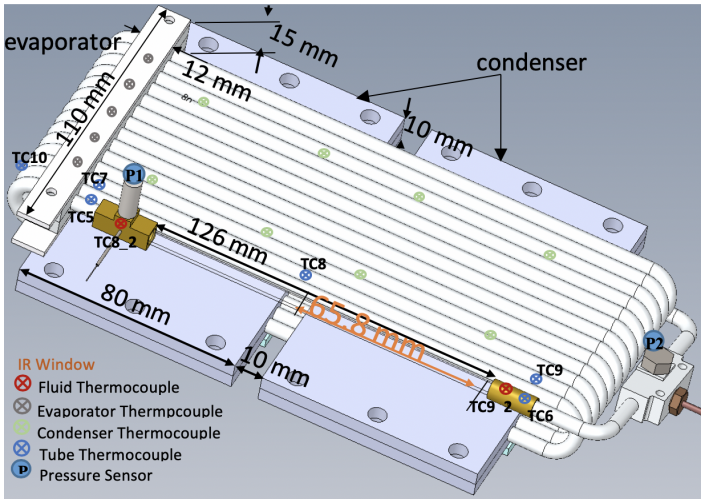

Figure 1. The tube temperature is measured with the thermocouples TC 5-TC10, while the fluid temperature, with the thermocouples TC8_2, TC9_2. The fluid pressure is measured with the pressure transducers P1, P2. Some of thermocouples are located inside the evaporator spreader block, some inside the condenser blocks. The size of the transparent PHP branch is shown together with the position and length of its portion observed with the IR camera (IR window) and with a high-speed grey-scale camera (Visible window).

At the ends of the sapphire tube, a pressure transducer and two K-type micro-thermocouples are installed inside the tube to measure the liquid temperature. Five T-type thermocouples are located between the evaporator spreader and heater; six are located between the Peltier cold side and the condenser spreader; two on top of the condenser spreader; seven are located on the tube external wall. The heating power is provided by a programmable power supply. The parabolic fligH campaign lasted three days, during each day thirty-one parabolic maneuvers have been performed: the first parabola was followed by six sequences of five consecutive parabolas; after each sequence a five minutes break of steady fligH was taken. Each parabola is a series of hyper-gravity period (20±2 s at 1.8g), micro-gravity period (20s±2 s at 0g), and again a hyper-gravity period. During the first two days, devoted to the thermal characterization, the device has been heated up at the desired temperature before the micro-gravity occurrence and the power was kept constant throughout each sequence. During the third day, devoted to the startup phenomena, the device has been heated up just after the occurrence of microgravity in order to prove that the incipience of the fluid motion is induced by the thermal effect and not by the inertial effects. To let the PHP equilibrate thermally at Tc, the power has not been switched during some parabolas. We discuss here only one (the 19th) parabola where the initial temperature was enough homogeneous and the plug flow was detectable in the transparent section. The flow and the temperature distribution in the transparent section have been detected by the analysis of the images obtained with the a long wave infrared (IR) camera (AIM®, bandwidth 3 – 5 μm, 1280x1024 pixels, resolution 40 μm). The method of analysis of the IR images is described in Catarsi et al. [3].

2.1. CASCO Simulations

The CASCO approach is 1D. The code is stable and computationally efficient: the simulation described below takes several minutes at the desktop PC. The specific PHP parameters

Evaporator length	12 mm
Lengths of condenser sections	80 mm, 80 mm
Length of adiabatic section	32 mm, 10 mm, 218 mm
Number of turns, Nturn	14
Length of the feed-back section	84 mm
Turn curvature radius	8 mm
Outer tube diameter, de	5 mm
Inner tube diameter, d	3 mm
Time step	0.1 ms
Tube mesh spacing	2 mm
Liquid mesh spacing (approximately)	1 mm
Parameters obtained by fitting to the experimental data	
Thermal mass of evaporator spreader, Cs	67 J/K
Contact thermal conductance, Us	1600 W/(m2K)
Liquid film thickness	72 μm
Vapor bubble nucleation barrier	5 K

used for the simulation are listed in Table 1. The PHP geometry (location and size of the evaporator, condenser and adiabatic sections, turn number, etc.) is that of Fig. 1. The structure of the PHP is specific, with three adiabatic sections per PHP turn as measured along the tube: between the evaporator and the 1st condenser, between two condensers, and between the 2nd condenser and the evaporator section of the next turn. Since the thermal gradients are measured to be extremely low in the spreader, it is assumed isothermal so its temperature Te depends only on time. It is found from the energy balance of the spreader

$$C_s \frac{\mathrm{d}T_e}{\mathrm{d}t} = P_e - \pi d_e \int q_s(x)\mathrm{d}x; \qquad q_s(x) = U_s[T_e - T_w(x)] \tag{1}$$

where $Cs = \rho_s V_s cp_s$ is the equivalent thermal mass of the spreader; ρ_s is the spreader density; V_s is the spreader volume; cp_s is the spreader heat capacity; P_e input power; d_e is the external tube diameter; q_s is the heat flux from the spreader to the tube; T_w is the tube wall temperature. Integration is performed over 14 evaporator sections of the tube. To adequately describe the empty PHP, it was necessary to introduce the contact thermal resistance between evaporator spreader and the tubes (with U_S, the contact thermal conductance). T_w is determined from the equation

$$\frac{\partial T_w}{\partial t} = D_w \frac{\partial^2 T_w}{\partial x^2} + \frac{j_w}{\rho_w c_w}; \qquad j_w = \frac{\pi}{S_w} \begin{cases} d_e q_s - dq_{fluid} & \text{if } x \in evaporator \\ -dq_{fluid} & \text{if } x \in adiab.\ sec. \end{cases} \tag{2}$$

where j_w is the effective power per unit volume; ρ_w is the tube density; c_w. is the tube heat capacity; $S_w$is the cross-section; d is the inner tube diameter; q_{fluid} is the wall to fluid heat flux defined in [4] and $S_w = 0.25\pi(d_e^2 - d^2)$. Note that the constant temperature $T_w = T_c$ is imposed within the condenser sections. The parameters C_s and U_s have been adjusted by using the experimental data on the empty PHP.

Unfortunately, the 20 s micro-gravity duration is too small to achieve a stable functioning regime so the transient simulation is required. The data are then dependent on the initial phase distribution, which is however unknown because the most of PHP is opaque. One can only reasonably guess that (i) the liquid gathers at the evaporator side due to the vertical favorable orientation of PHP during the hyper-gravity period preceding micro-gravity and

(ii) the internal tube walls are covered by a continuous liquid film formed during preceding parabolas.

3. Results and discussion

Comparisons of the tube wall and evaporator temperatures measured experimentally and simulated with CASCO are presented in Figures 2 - 8. The agreement is very good. The velocities of liquid plugs (Figures 9 and 10) are also quite similar. In the case of Figure 9, the simulation captures closely the evolution for t <5 s. For t >5 the velocity modulus is reproduced, but not the sign. The reason is the unknown initial phase distribution inside the tube. Similar results are obtained for the case in Figure 10. In Figures 11 and 12the comparison of liquid slugs lengths in showed. color correspond to a specific liquid plug appearing in the transparent section during the start-up; in both cases there is a qualitative agreement. Finally Figures 13 and 14there are shown respectively the experimental and simulation temperature distribution on liquid slugs; one can see the sharp temperature variation near the menisci both in the experimental and simulation data. For the first time in the literature, at least to the authors' knowledge, a multi-parametric transient comparison has been done quantitatively on several physical variables such as fluid and wall temperatures and slug lengths and velocities and the agreement of the experimental and simulation data is satisfactory.

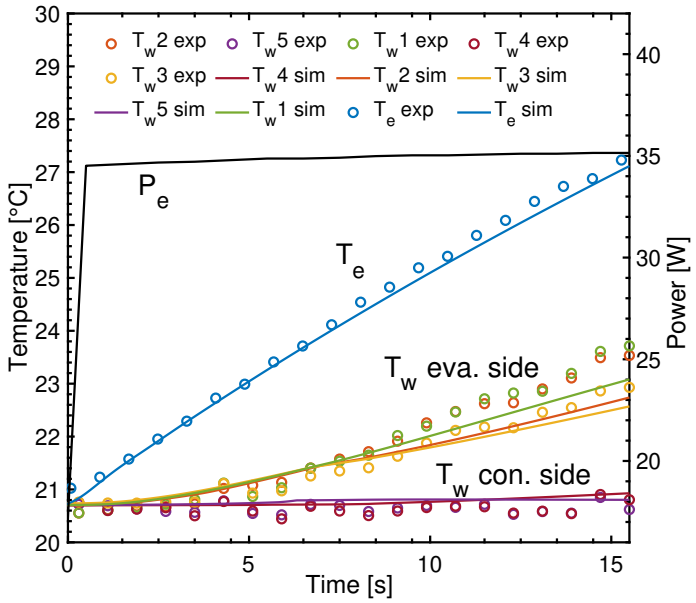

Figure 2. Parabola 2 temperature evolution. Input Power 35 W

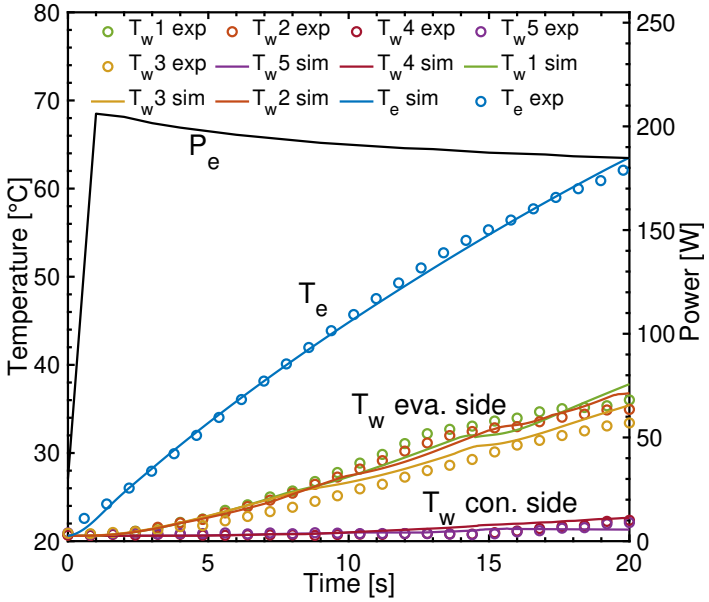

Figure 3. Parabola 19 temperature evolution. Input Power 205 W

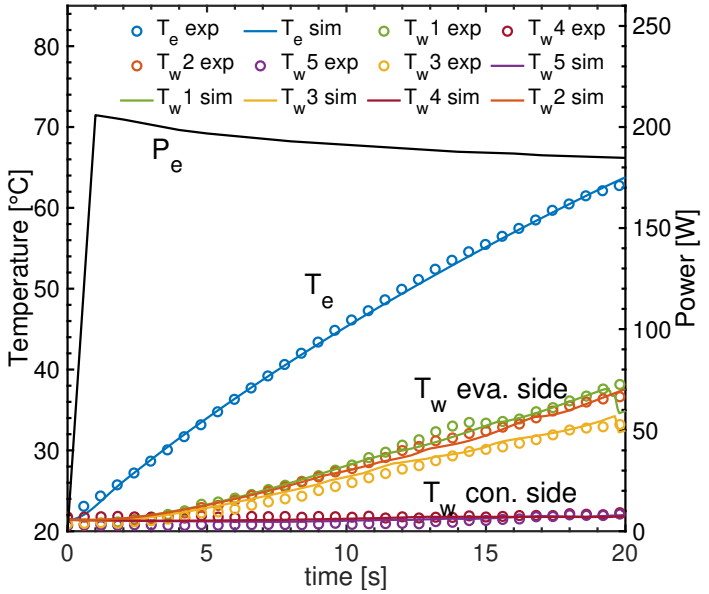

Figure 4. Parabola 16 temperature evolution. Input Power 200 W

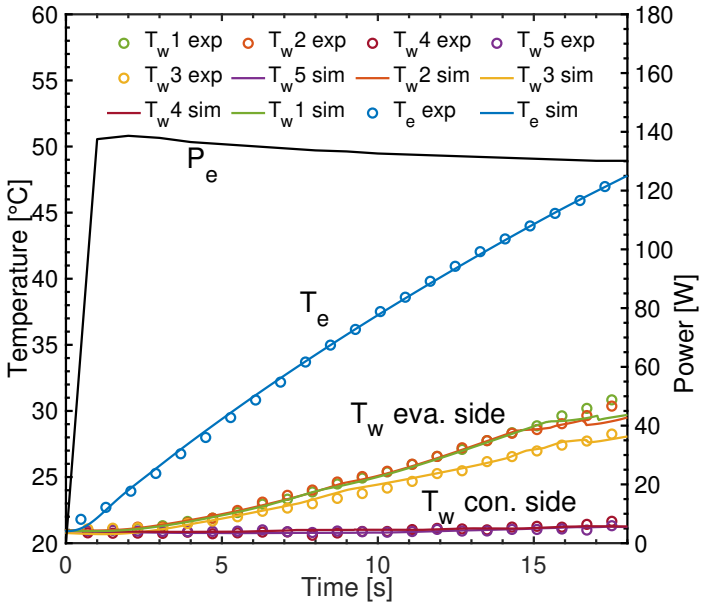

Figure 5. Parabola 22 temperature evolution. Input Power 135 W

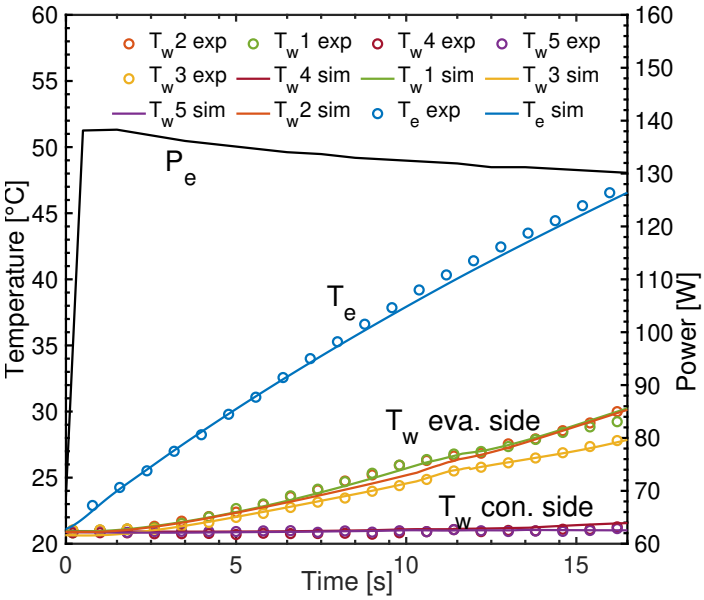

Figure 6. Parabola 25 temperature evolution. Input Power 135 W

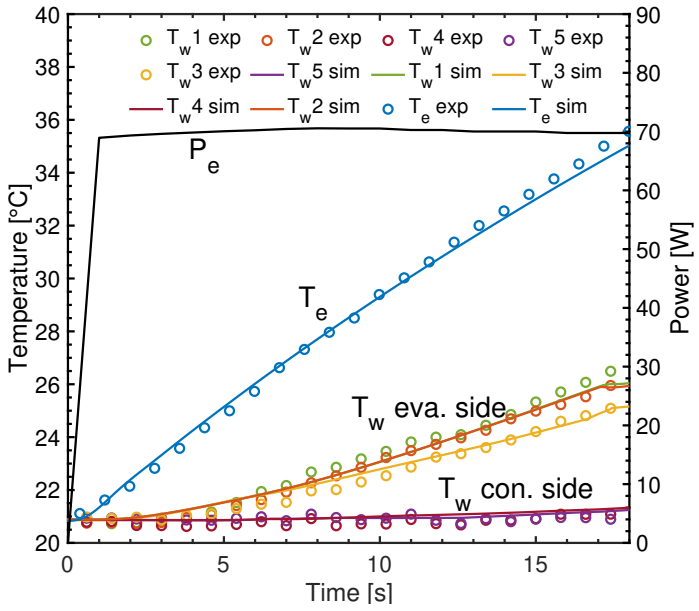

Figure 7. Parabola 27 temperature evolution. Input Power 70 W

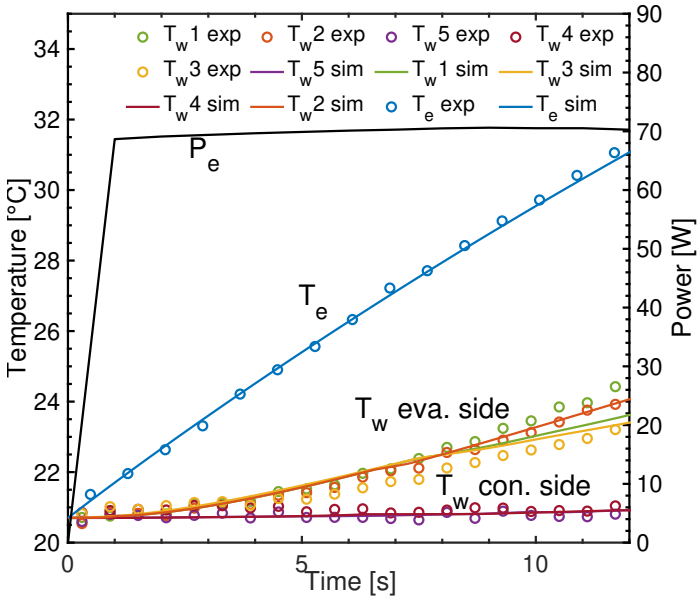

Figure 8. Parabola 30 temperature evolution. Input Power 70 W

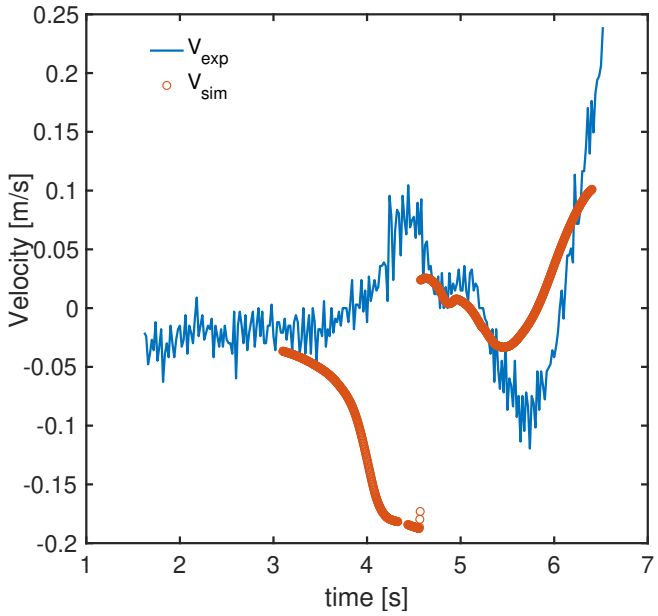

Figure 9. Temporal evolution of liquid slugs velocity during parabola 19. Experimental velocity in blue; simulated velocity in orange.

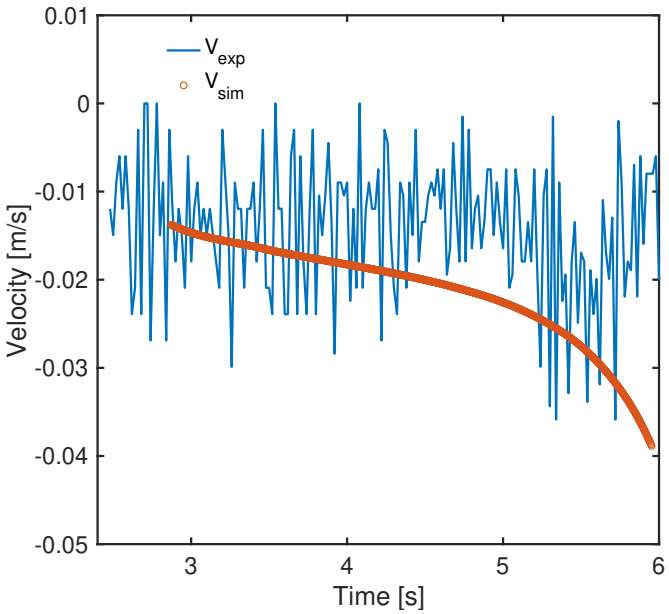

Figure 10. Temporal evolution of liquid slugs velocity during parabola 30. Experimental velocity in blue; simulated velocity in orange.

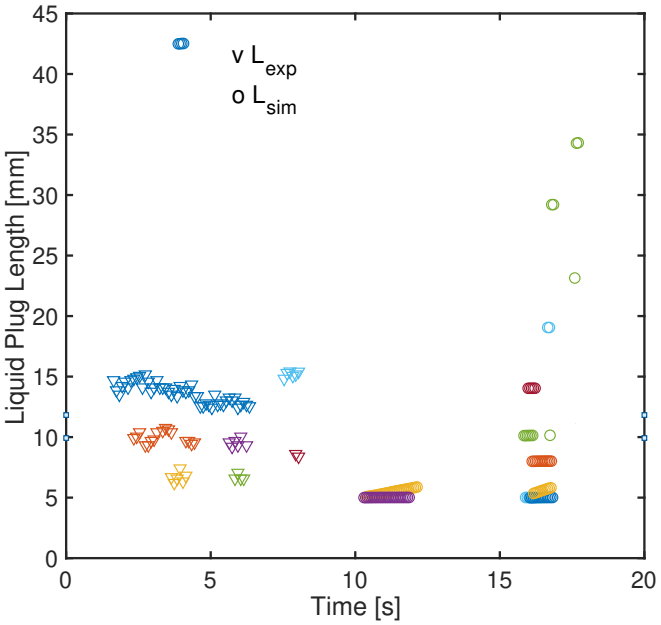

Figure 11. Evolution of liquid slugs length during parabola 19. Experimental lengths in cross markers; simulated lengths in circular markers.

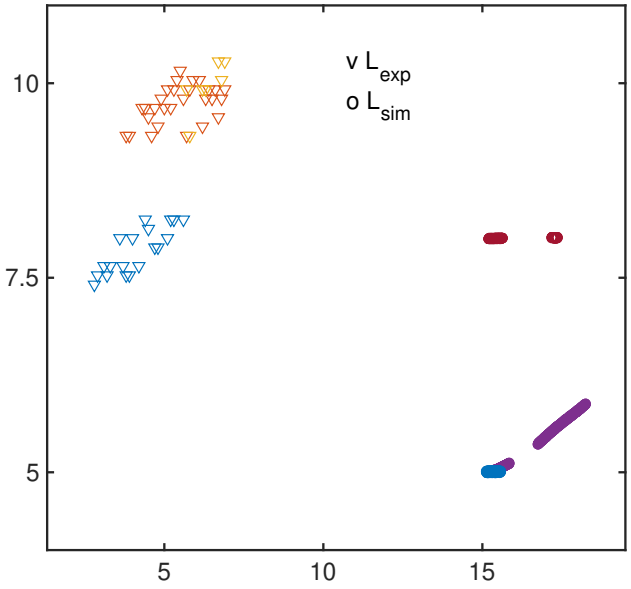

Figure 12. Evolution of liquid slugs length during parabola 30. Experimental lengths in cross markers; simulated lengths in circular markers.

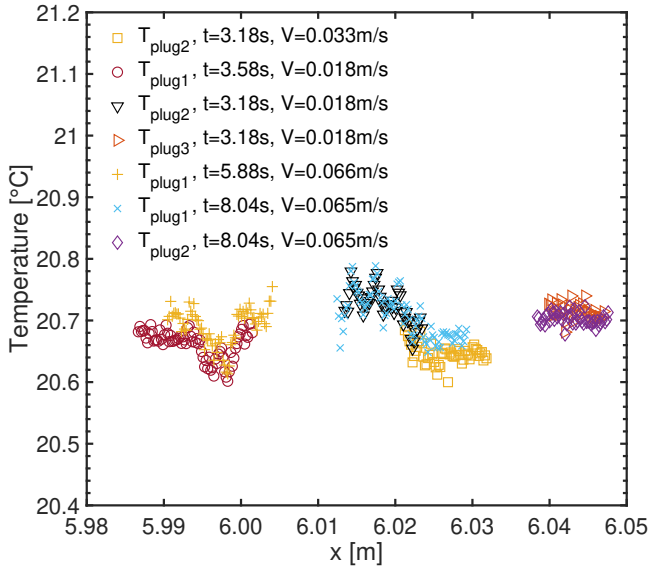

Figure 13. Experimental liquid slugs temperature distribution during parabola 19

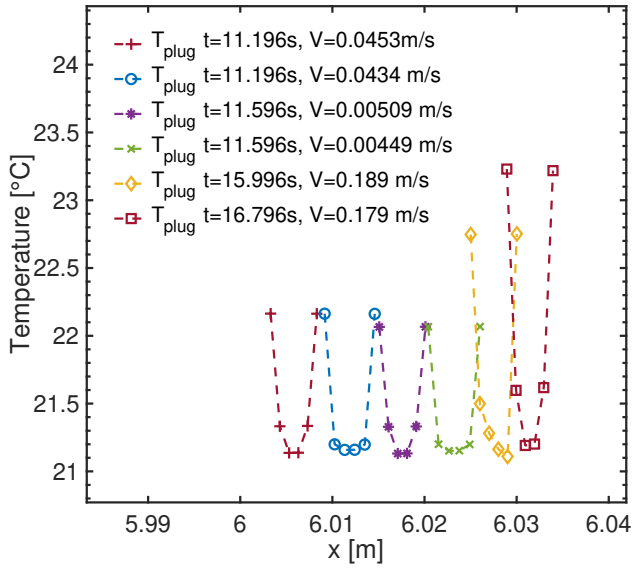

Figure 14. Simulation liquid slugs temperature distribution during parabola 19

Acknowledgments

References

[1] Gu J, Kawaji M and Futamata R 2005 *Microgravity Science and Technology* **15** 181

[2] Daimaru T, Nagai H, Ando M, Tanaka K, Okamoto A and Sugita H 2017 *Int. J. Heat Mass Transf.* **109** 791 URL `http://dx.doi.org/10.1016/j.ijheatmasstransfer.2017.01.078`

[3] Catarsi A, Fioriti A, Mameli M, Filippeschi S and Di Marco P 2018 *Proceedings of the 16th International Heat Transfer Conference* (Beijing, China)

[4] Nikolayev VS 2011 *Journal of Heat Transfer* **133** 081504

[5] Nekrashevych I and Nikolayev VS 2017 *Applied Thermal Engineering* **117** 24

[6] Nikolayev VS and Marengo M 2018 Modeling of Two-Phase Flows and Heat Transfer